Military Technical College
Kobry El-Kobba,
Cairo, Egypt

11-th International Conference
on Aerospace Sciences &
Aviation Technology

A RELIABILITY MEASURE FOR ESM SYSTEM DEINTERLEAVERS

*Dr. Hossam E. Abou-Bakr Hassan

ABSTRACT

An Electronic Support Measures (*ESM*) system consists principally of a passive radar receiver and a deinterleaver. It measures the monopulse parameters of intercepted radars, sorts them into individual radars, identifies those radars, and passes their identities to an Electronic Counter Measures (*ECM*) system for further action. When the pulse arrival rate is too high for an *ESM* system, it will skip some pulses and consequently the reliability of radar identification will be decreased. From queueing theory, this paper develops an expression that relates the reliability, quantified as a figure of merit called the factor of successful processing (F_s), to the pulse arrival rate and the service times of the *ESM* system. An on-line method to measure F_s is also given, which shows that the measurements are in close agreement with the theoretical values.

1. INTRODUCTION

An Electronic Support Measures (*ESM*) system [1,2] consists of a passive radar receiver, a deinterleaver that sorts an intercepted pulse stream into individual sequences and then measures the radar parameters for identification. An *ESM* block diagram is in Figure 1.

For each incoming pulse, the Receiver-Encoder (R-E) measures its Angle of Arrival (*AOA*), Radio Frequency (*RF*), Pulse Amplitude (*PA*), Pulse Width (*PW*) and Time of Arrival (*TOA*). The *AOA* and *TOA* are the more accurate pulse parameter. A *PDV* (Pulse Descriptor Vector or Word) that contains these parameters in a digital format then goes to the preliminary deinterleaver, which separates these PDVs into streams that have common *AOA* and *RF*. Typically in a dense environment, a stream may contains *PDVs* of up to five different radars. The final deinterleaver then must separate these *PDVs* to produce Emitter Descriptor Vector (*EDV*), that contains AOA, RF, PA, PW from PDVs,

* Egyptian Armed Forces

and additional parameters such as Pulse Repetition Interval (*PRI*), agility and scan period. The identifier next attempts to match an *EDV* with those in the reference library so that an Electronic Counter Measures (*ECM*) system can generate actions against a particular radar. It is noted that the above is a very cursory description of the *ESM-ECM* functions, which in general are very complex.

When the pulse arrival rate is too high for the *ESM* system, overlapping occurs. Thus when the time between pulses is shorter than the time it takes the R-E to measure the *PDV*, the R-E will miss pulses. Similarly, if the time between *PDVs* is faster than the assignment time T_a of the deinterleaver, it will miss some *PDVs*. It is of practical interest to determine the relationship between the pulse arrival rate and the *PDV* assignment (to *EDVs*) rate. Let this be the factor of successful processing F_S. It is the product of F_P and F_E, where for any time period T,

$$F_P = \frac{number\ of\ PDVs\ emerging\ from\ R-E\ over\ T}{number\ of\ pulses\ arriving\ over\ T} \tag{1}$$

$$F_E = \frac{number\ of\ PDVs\ assigned\ to\ EDVs\ over\ T}{number\ of\ PDVs\ emerging\ from\ R-E\ over\ T} \tag{2}$$

$$F_s = F_P F_E = \frac{number\ of\ PDVs\ assigned\ to\ EDVs\ over\ T}{number\ of\ pulses\ arriving\ over\ T} \tag{3}$$

and is a measure of the number of pulses that successfully receives *EDV* assignment. Conversely, $1\text{-}F_S$ is a fraction that represents the number of pulses that misses assignment, due either to blocking in the R-E or the deinterleaver.

This paper first derives equation for the fractions F_P and F_E and then F_S, as a function of the R-E service time T_S and the deinterleaver assignment time T_a, and the pulse arrival rate. It then moves on to give a method for measuring on-line the number of missing pulses, and consequently F_S, from the output of the deinterleaver. There are two important reasons to know when the *ESM* system is missing pulses and by how many. First, too many missing pulses in an *EDV* will reduce its reliability, and the *ESM* system should not pass inaccurate *EDVs* to an *ECM* system, in order to avoid wrong tasking. Second, a large number of missing pulses signals that the system is overloading, and requires additional processing capacity.

While there are papers [2,5,6] on the topic of deinterleaving, there is no reference in the open literature that deals with the assessment of the reliability of the identification from an *ESM* system.

The organization of the paper is as follows. Sections 2 and 3 contain, respectively, the development of the equation for F_P and F_E. Section 4

describes the process of histogramming of *TOAs* to estimate *PRI*, followed by Section 5, which gives an on-line measurement method for F_S. The simulation results are in Section 6. The simulation experiments serve to verify the theoretical development for F_P and F_E, and they also show good agreement between the theoretical and on-line F_S. The conclusions are in Section 7.

2. DERIVATION OF F_P

The fraction of pulse completion in (1) is the ratio, over a period T, of the number of pulses that the R-E processes to the number of pulse arriving and $F_P \leq 1$. An $F_P < 1$ indicates that the pulse arrival rate is too fast for the service time T_s of the R-E so that it skips the processing of some pulses. Similarly, the fraction of *PDV* assignment completion in (2), F_E, if <1, signals that the *PDV* arrival rate is too fast for deinterleaver assignment time T_a.

This section and the follow develop, from queueing theory, expression for F_P and F_E, as functions of T_s and T_a and the pulse arrival rate. In a dense emitter environment, the *TDOA* between successive pulses at the *ESM* receiver input is an exponentially distributed random variable with parameter λ, where λ [1] is the arrival rate of pulses at the input of the *ESM* receiver. Thus, the probability density function (*pdf*) of the *TDOA* is

$$f_T(t) = \lambda e^{-\lambda t} \tag{4}$$

The service time inside the *ESM* receiver is a fixed value denoted by T_s. This time is selected to be the maximum expected *PW* among the intercepted pulses. The fraction of pulse completion is then the fraction of the arriving pulses that are separated in time by T_s or more. This value is denoted by F_P and is given by

$$F_P = \int_{T_s}^{\infty} \lambda . e^{-\lambda t} dt = e^{-\lambda . T_s} \tag{5}$$

A computer program is developed to corroborate the theoretical development through the paper. First we simulate an *ESM* system environment consisting of several radars. The *AOA*, *RF*, *PW* and *PRI* and the variations of these parameters of each radar are described. The program assigns a random start time to each radar and then calculates the position of the successive pulses from that radar according to its *PRI* mode and its *PRI* value(s). The parameters of every pulse from radars present in the environment of the *ESM* system are slightly modified by adding measurement errors to increase the realism of the simulations. Each received pulse at the input of the *ESM* system is represented as a vector (*PDV*), whose elements are the *AOA*, *RF*, *PW* and *TOA* of this pulse. The received pulses from all radars present in the environment of the

ESM system during the given observation time are sorted in ascending order with respect to their *TOAs*. This leads to generating a stream of interleaved radar pulses from different radars.

The pulse with the smallest *TOA* is considered as the first pulse being processed by the *ESM* receiver. The processing (service) time in the *ESM* receiver is constant. Hence, the *ESM* receiver can only process a pulse, which arrives after a constant service time from the previous processed pulse. The ratio between the number of pulses that are being processed in the *ESM* receiver to the number of arriving pulses at the input of the *ESM* receiver is the fraction of pulse completion, which is derived analytically in this Section.

The *PDVs* emerge from the *ESM* receiver to the deinterleaver are sorted, segregated and assigned to one of the *EDVs*. A *PDV* will be blocked from being assigned to one of the radar cells when the deinterleaver is busy in processing another one and there is no waiting room for this *PDV*. The ratio between the *PDVs* that are successfully assigned to the *PDVs* that emerged from the *ESM* receiver is the fraction of *PDV* assignment completion which is derived analytically in Section III. After segregating the *PDVs*, we apply the method presented in Section V to evaluate quality of each deinterleaved and calculate F_S on-line.

In this Section, the simulation program is performed for different pulse rates at the input of the *ESM* receiver. During a given time interval, we divide the number of *PDVs* emerging from the *ESM* receiver by the number of pulses arriving at the input of the *ESM* receiver. This fraction is denoted as $\hat{F}_P$ and it is compared with F_P for different services times T_S. We present this comparison in Figure 2.

3. DERIVATION OF F_E

3. 1. Equation for F_E

The deinterleaver next sorts the *PDVs* and forms pulse cells assumed to belong to the same emitter. The time needed to assign an incoming *PDV* to one of the generated cells is a constant and denoted by T_a. It is worth noting that the performance of the deinterleaver will improve when it has a pre-buffer of size *K* [2]. The function of the pre-buffer is to store up to *K* of the arriving *PDVs* when the deinterleaver is busy. In this section we develop an expression for the fraction of *PDV* assignment completion (F_E).

Suppose the deinterleaver is preceded by a pre-buffer of size *K*. The instant at which the deinterleaver completes servicing the n^{th} *PDV* is the instant when the deinterleaver is ready to service the $(n+1)^{th}$ *PDV*. Let us designate the state of the deinterleaver by a positive integer *k*, where *k* is the number of *PDVs* inside the deinterleaver and the pre-buffer. Now we denote the probability that the

state of the deinterleaver is k by π_k, $0 \leq k \leq K+1$. The probability that j *PDVs* arriving at the input of the deinterleaver during the service time of a given *PDV* is denoted by r_j. It can be [8-10] deduced that

$$\pi_i = \pi_0 r_i + \sum_{j=1}^{i+1} \pi_j r_{i-j+1} \; ; \; i = 0, 1, 2, \ldots\ldots, K \tag{6}$$

The above system can be solved for $\pi_1, \pi_2, \ldots\ldots, \pi_i, \ldots\ldots, \pi_{K+1}$ in terms of π_0. For this purpose it is enough to consider the first K equations of (6). They can be solved by the forward substitution algorithm [11]. By imposing the constraint $\sum_{i=0}^{K+1} \pi_i = 1$, the value of π_0 and hence the values of the other probabilities π_k, $1 \leq k \leq K+1$ can be determined. It is found that (6) can also be solved in a recursive way as follows. Let us define the following system of equations

$$C(0)=1 \tag{7}$$

$$C(i+1) = \frac{C(i) - \left[C(0) r_i + \sum_{j=1}^{i} C(j) r_{i+1-j} \right]}{r_0}, \; i = 1, 2, \ldots\ldots, K \tag{8}$$

From (7) and (8) π_k, $0 \leq k \leq K+1$ can be calculated as follows

$$\pi_0 = \frac{1}{\sum_{i=0}^{K+1} C(i)} \tag{9}$$

$$\pi_i = C(i) \pi_0 \tag{10}$$

The fraction of *PDV* assignment completion (F_E) is simply the ratio of the rate of the processed *PDVs* to the rate of input *PDVs*. The rate of the processed *PDV* is the reciprocal of the expected value of the times between *PDVs* from the deinterleaver. The time between the output *PDVs* from the deinterleaver takes one of the following values:

T_a when there is one *PDV* or more in the deinterleaver and the pre-buffer in addition to the current processed *PDV*. The same value is obtained when there is no *PDV* in the deinterleaver and the pre-buffer except the currently processed *PDV* and one or more *PDVs* arrives at the deinterleaver input during the service time (T_a) of the current processed *PDV*.

T_a + 1/ λ_0, where λ_0 is the average rate of incoming *PDVs*, when there is no *PDV* in the deinterleaver and the pre-buffer except the currently processed *PDV* and no *PDV* arrives at the deinterleaver input during the processing time of the current *PDV*.

The expected time between *PDVs* from the deinterleaver is then

$$\overline{T_{out}} = \mathbf{T}_a\left[(1-\pi_0)+(\pi_0(1-r_0))\right]+\left(\mathbf{T}_a+\left(\frac{\mathbf{1}}{\boldsymbol{\lambda_0}}\right)\right)[\pi_0 r_0] \tag{11}$$

Consequently, the fraction of successfully processed *PDVs* is

$$F_E = \begin{cases} \dfrac{1}{\overline{T_{out}}\lambda_0} & \lambda_0 \geq \dfrac{1}{\overline{T_{out}}} \\ 1 & Otherwise \end{cases} \tag{12}$$

As seen in (11) and (12), F_E is a function of the rate of the incoming *PDVs* and the probabilities π_0 and r_0. In (8) to (10), r_j, $0 \leq j \leq K$ are required in order to find π_0 and r_0. Therefore, we will derive in the following subsections the expressions for λ_0 and the probabilities r_j, $0 \leq j \leq K$.

3. 2. The Rate of PDVs

The departure process of *PDVs* from the *ESM* receiver is a renewal process [1, 12] since the pulses of the input flow, which are blocked, are not randomly selected. The departure process has therefore a residual effect and is not a Poisson process. The distribution of the interdeparture times between successfully processed pulses is deduced [12] from the *TDOA* of pulses as follows.

$$f_{T_d}(l)\Delta l = \frac{proportion\ of\ \text{TDOA times in}\ the\ range(l, l+\Delta l)}{proportion\ of\ the\ TDOA\ times\ in\ excess\ of\ T_s}$$

$$= \frac{\int_{l}^{l+\Delta l}\lambda e^{-\lambda t}dt}{\int_{T_s}^{\infty}\lambda e^{-\lambda t}dt} = \frac{e^{-\lambda l}-e^{-\lambda(l+\Delta l)}}{e^{-\lambda T_s}} = \frac{e^{-\lambda l}\left(1-e^{-\Delta l}\right)}{e^{-\lambda T_s}} = \frac{e^{-\lambda l}\left(1-(1-\lambda\Delta l)\right)}{e^{-\lambda T_s}} = \frac{e^{-\lambda l}\lambda.\Delta l}{e^{-\lambda T_s}} \tag{13}$$

From (13), it is clear that

$$f_{T_d}(l) = \lambda e^{-\lambda(l-T_s)};\ \ l \geq T_s \tag{14}$$

where T_d is the interdeparture time between the output *PDVs*. The rate of *PDVs* arriving at the input of the deinterleaver is the reciprocal of the expected value of the interdeparture times between *PDVs* at the output of the *ESM* receiver. From (16), the expected value of the interdeparture times is

$$\overline{T_d} = \int_{T_s}^{\infty} t\lambda e^{-\lambda(t-T_s)}dt = T_s + \frac{1}{\lambda} \tag{15}$$

Consequently the average rate of *PDVs* at the input of the deinterleaver is

$$\lambda_0 = \frac{1}{\overline{T_d}} = \frac{\lambda}{1+\lambda.T_s} \tag{16}$$

In the next subsection a formula for the probabilities r_j, $0 \le j \le K$, based on the departure process of *PDVs* from the *ESM* receiver and the assignment time inside the deinterleaver, T_a will be derived.

3. 3. Calculation of the Probabilities $\{r_j\}$

To derive a formula for the probabilities $\{r_j\}$, the cumulative distribution function (*CDF*), of the departure counting process from the ESM receiver is calculated. The *CDF* = R_j, is the probability that the number of *PDVs* emerging from the *ESM* receiver during the service time of the deinterleaver T_a, is smaller than or equal to *j*. Then, the probability r_j is given by

$$r_j(T_a) = \begin{cases} R_j(T_a) - R_{j-1}(T_a), & j \ge 1 \\ R_j(T_a) & j = 0 \end{cases} \tag{17}$$

But

$$R_j(t) = \Pr obability\{(\text{sum } of\ j+1\ departure\ times\ from\ the\ ESM\ receiver) > t\} \tag{18}$$

Thus, an expression for the *pdf* of a random variable consisting of the sum of independent, identically distributed random variables all having the *pdf* defined in (14) have to be deriven.

It is known [8-10] that if T_{d_1}, T_{d_2}, ..., T_{d_i}, ..., T_{d_N} are *N* independent identically distributed random variables having the same *pdf*, $f_{T_{d_i}}(t)$, then the *pdf* of a new random variable $T = \sum_{i=1}^{N} T_{d_i}$ is given by

$$f_T(t) = f_{T_{d_1}}(t) * f_{T_{d_2}}(t) * ..... * f_{T_{d_i}}(t) * ..... * f_{T_{d_N}}(t) \tag{19}$$

Taking the Laplace transform of both sides of (19), we have

$$L(f_T(t)) = L\left(f_{T_{d_1}}(t) * f_{T_{d_2}}(t) * \ldots\ldots * f_{T_{d_i}}(t) * \ldots\ldots * f_{T_{d_N}}(t)\right) \tag{20}$$

which leads to

$$L(f_T(t)) = \prod_{i=1}^{N} L\left(f_{T_{d_i}}\right) \tag{21}$$

In our case, $f_{T_{d_i}}(t) = \lambda e^{-\lambda(t-T_s)}; t \geq T_s$, and its Laplace transform is given by

$$L\left(f_{T_{d_i}}(t)\right) = \int_{T_s}^{\infty} \lambda e^{-\lambda(t-T_s)} e^{-st} dt = \frac{\lambda}{\lambda + s} e^{-sT_s} \tag{22}$$

Therefore,

$$L(f_T(t)) = \left(\frac{\lambda}{\lambda + s} e^{-sT_s}\right)^N \tag{23}$$

The *pdf* of $f_T(t)$ is obtained by calculating the inverse Laplace transform of (23)

$$f_T(t) = L^{-1}\left[\left(\frac{\lambda}{\lambda + s} e^{-sT_s}\right)^N\right]$$
$$= \frac{\lambda\left(\lambda\left(t - NT_s\right)\right)^{N-1}}{(N-1)!} e^{-\lambda(t-NT_s)} \tag{24}$$

which is the probability of the sum of *(j+1)* interdeparture times equal to *t*. Then R_j can be calculated as

$$R_j(t) = \int_t^{\infty} \frac{\lambda\left(\lambda\left(x - (j+1)T_s\right)\right)^j}{j!} e^{-\lambda\left(x-(j+1)T_s\right)} dx \tag{25}$$

Letting $u = x\text{-}t$ gives

$$R_j(t) = \int_0^{\infty} \frac{\lambda^{j+1}\left(u + t - (j+1)T_s\right)^j}{j!} e^{-\lambda(u+t-(j+1)T_s)} du$$

$$= e^{(j+1)\lambda T_s} \int_0^{\infty} \frac{\lambda^{j+1} e^{-\lambda t} e^{-\lambda u}}{j!} \sum_{i=0}^{j} \frac{u^{j-i}\left(t - (j+1)T_s\right)^i j!}{i!(j-i)!} du \tag{26}$$

by using the binomial series expansion. Interchanging the order of integration and summation yields

$$R_j(t) = e^{(j+1)\lambda T_s} \sum_{i=0}^{j} \frac{\lambda^{j+1} e^{-\lambda t} \left(t-(j+1)T_s\right)^i}{i!(j-i)!} \int_0^\infty e^{-\lambda u} u^{j-i} du \qquad (27)$$

But $\int_0^\infty e^{-u} u^{j-i} du$ is the well-known gamma function denoted by $\Gamma(j\text{-}i+1)$ which is equal to $(j\text{-}i)!$. Thus with the proper change of variables to account for λ in $e^{-\lambda u}$, we get

$$R_j(t) = e^{\lambda(j+1)T_s} \sum_{i=0}^{j} \frac{\left(\lambda\left(t-(j+1)T_s\right)\right)^i}{i!} e^{-\lambda t} \qquad (28)$$

Consequently, the probabilities r_j; $0 \le j \le K$ in (17) can be calculated and will yield the fraction of *PDV* assignment completion F_E after substitution into (11) and (12).

3. 3. Validation of the Derived Formula of F_E

The simulation of the operation of the *ESM* system for different numbers of radars have been performed and hence, different pulse arrival rates. By dividing the number of *PDVs* that are successfully assigned to the generated radar cells by the number of *PDVs* arriving at the input of the deinterleaver during a given time interval, we obtain $\hat{F}_E$. For the same *ESM* parameters (T_s, T_a, *pre-buffer size=K*), and arrival rate λ, we calculate the fraction of *PDV* assignment completion or ratio of successfully processed *PDVs* by using (12). This value is denoted as F_E. In the following tables we present $\hat{F}_E$ and F_E for different values of the parameters and different pulse rates at the input of the *ESM* system.

Table 1. The fraction of *PDV* assignment completion as a function of T_s *and* T_a with arrival rate = 23990 Pulse/sec. , *pre-buffer size =5 PDVs.*

		T_a 50[μsec.]		T_a 54[μsec.]		T_a 58[μsec.]		T_a 62[μsec.]		T_a 66[μsec.]		T_a 70[μsec.]	
		$\widehat{F}_E$	F_E	$\widehat{F}_E$	F_E	$\widehat{F}_E$	F_E	$\widehat{F}_E$	F_E	$\widehat{F}_E$	F_E	$\widehat{F}_E$	F_E
λ = 23990 [Pulse/sec.]	T_s= 2 μ sec.	86.9	86.5	80.5	80.5	74.7	75.1	70.1	70.4	65.9	66.1	62.3	62.3
	T_s= 4 μ sec.	90.5	89.6	83.6	83.9	77.9	78.5	72.8	73.5	68.1	69.1	64.3	65.2
	T_s= 7 μ sec.	95.3	93.2	88.0	88.2	82.3	83.1	76.9	78.2	72.2	73.6	67.9	69.5

As seen in Table 1, there is an excellent agreement between $\widehat{F}_E$ and F_E. Moreover, for the given arrival rate of pulses at the input of the *ESM* receiver and T_s we can see that as T_a increases, the fraction of *PDV* assignment completion decreases. More importantly, for a given arrival rate of pulses and T_a, as T_s increases, the fraction of *PDV* assignment completion increases. This happened because the fraction of *PDV* assignment completion increases as the rate of *PDVs* at the input of the deinterleaver decreases, and this rate given by (18) as an inverse function of T_s. In the following Table, we present the fraction of *PDV* assignment completion as a function of the pulse rate.

Table 2. The fraction of PDV assignment completion as a function *of* λ, T_s = 3 μsec. , *pre-buffer size = 5 PDVs.*

		T_a 60[μsec.]		T_a 62[μsec.]		T_a 64[μsec.]		T_a 66[μsec.]		T_a 68[μsec.]	
		$\widehat{F}_E$	F_E	$\widehat{F}_E$	F_E	$\widehat{F}_E$	F_E	$\widehat{F}_E$	F_E	$\widehat{F}_E$	F_E
T_s = 3 μsec.	λ[P/sec.] 16920	99.5	98.8	98.5	96.6	95.8	94.4	92.4	92.1	89.9	89.8
	λ[P/sec.] 17860	96.9	95.3	93.3	92.9	90.9	90.5	87,8	88.2	84.9	85.9
	λ[P/sec.] 18820	91.8	91.6	88.7	89.2	86.6	86.7	83.4	84.4	81.0	82.1

As seen in Table 2, there is an excellent agreement between $\hat{F}_E$ and F_E. A new observation obtained from Table 1 besides those obtained from Table 2 is that for the given T_s and T_a the function of *PDV* assignment completion decreases as the arrival rate increases.

4. HISTOGRAM PATTERNS

To find the theoretical F_s obtained in Section III requires the knowledge of λ, the pulse arrival rate, λ_0, the *PDV* arrival rate, and the probabilities $\pi_k(t_n)$ and r_j, which depend on the deinterleaver state

Measuring these values on-line will be difficult, if not impossible. But since F_s is a function of the number of missing values, it may be able to measure F_s through that number. This Section provides an ad hoc approach to measure F_s. The basic assumption is that if the *ESM* system misses a pulse, it is due strictly to blockage. First, we examine how the deinterleaver forms histograms from the *TOAs* and how different radar types exhibit different histogram patterns.

4. 1. Stable *PRI* Radars

Consider a radar with a constant *PRI* = T_1. The ESM system receives the following emissions from this radar during the observation time θ. An ideal deinterleaver will place all received pulses in Figure 3 into a single cell. Ideal means that no pulse is missing and no pulse from other radars is added.

The difference between the *TOA* of the i^{th} pulse and the *TOA* of the $(i+1)^{th}$ pulse is defined as Δ_i. The Δ_i can be all different but usually, many of them will have the same values. For a stable radar with a *PRI* = T_1, the ideal deinterleaver will have one peak at $\Delta_i = T_1$ in the histogram representing the count of Δ_i as shown in Figure 4. The value of this peak is

$$hist(\Delta = T_1) = \frac{\theta}{T_1} \tag{29}$$

4. 2. Jittered *PRI* Radars

A jittered *PRI* changes its *PRI* randomly between two fixed bounds. Thus, there will be different Δ_i values between successive pulses inside the pulse train as shown in Figure 5. The jitter width δ is the larger of the difference between the high or the low bound and $\overline{PRI}$, the mean *PRI*. For a jittered *PRI*, the histogram bar is centered at $\overline{PRI}$ with a width equal to 2δ as shown in Figure 6. A *PRI* with a value Δ_i belongs to that bar if

$$\left|\overline{PRI} - \Delta_i\right| \le \delta \qquad i = 1,2,\ldots\ldots N \tag{30}$$

Figure 6 represents a histogram of the different values of Δ_i .The total number of Δ_i belonging to the histogram bar centered at $\overline{PRI}$ with a width of 2δ is

$$hist\left(\Delta = \overline{PRI}\right) = \frac{\theta}{\overline{PRI}} \tag{31}$$

4. 3. Staggered *PRI* Radars

The staggered *PRI* radar emits pulses with different *PRI* values repeated in a fixed sequence as shown, for example for three different *PRIs*, in Figure 7.
For the staggered *PRI* radar of Figure 8, Δ_i takes one of three values PRI_1, PRI_2 and PRI_3. The Δ histogram has three peaks at these three values as shown in Figure 8. The value of these peaks is

$$hist\left(\Delta = PRI_1\right) \cong hist\left(\Delta = PRI_2\right) \cong hist\left(\Delta = PRI_3\right) \cong \frac{\theta}{\sum_{i=1}^{3} PRI_i} \tag{32}$$

5. MEASUREMENT OF F_S ON-LINE

Equations (29), (30), and (31) are satisfied only if the deinterleaver is ideal. In a real situation, a number of pulses may be missing from an estimated radar cell or pulses from different radars are merged to form a new cell. This may be caused by: (a) the high pulse density in the *ESM* environment, which results in the time overlapping of received pulses, (b) the inaccuracy in measuring the monopulse parameters of each intercepted pulse, which leads to the insertion of the pulse into an incorrect cell, and (c) the deinterleaver not being able to keep up with the high pulse arrival rate. Thus, it is necessary to determine the reliability of each deinterleaved cell so that the *ESM* system can evaluate the performance of the deinterleaving process. In this Section we will present a method to estimate the number of missing pulses in each cell, leading to a formula for F_s, the factor of successful processing.

A figure of merit is determined for each estimated radar cell as follows [7]. Suppose that during an observation time θ, an estimated radar cell contains N different values of Δ_i denoted each by $\boldsymbol{d}_i$ with corresponding *hist* (d_i). Vectors $\boldsymbol{d}$ and ***hist*** are formed as follows.

$$\mathbf{d} = \left[d_1 \quad d_2 \quad . \quad . \quad d_N\right]^T, \quad \mathbf{hist} = \left[hist(d_1) \quad hist(d_2) \quad . \quad . \quad hist(d_N)\right]^T \tag{33}$$

A new vector **hist'** is obtained by dividing all elements of the vector **hist** by the largest element. If *hist* (d_j) is the largest, then **hist'** becomes

$$\mathbf{hist}' = \left[\frac{hist(d_1)}{hist(d_j)} \quad . \quad . \quad \frac{hist(d_j)}{hist(d_j)} \quad . \quad . \quad \frac{hist(d_N)}{hist(d_j)} \right]^T \tag{34}$$

Clearly, the largest element of **hist'** is 1. Next, elements of **hist'** smaller than a given threshold, and the corresponding elements in **d** are eliminated. This gives new vectors $\mathbf{d}_1$ and $\mathbf{hist}_1$ with dimension $N_1 \times 1$ where $1 \leq N_1 \leq N$.

The number of missing pulses in each cell can be estimated as follows. First, add all the elements in the vector $\mathbf{d}_1$. The sum is called PRI_{Frame}. For an ideal deinterleaver, with an equal number of *TOA* differences corresponding to each *PRI*, the total number of pulses in the observation time θ is

$$N_{Ideal} \approx N_1 \times \left[\frac{\theta}{PRI_{Frame}} + 1 \right] \tag{35}$$

In a real situation, there will be a number of pulses missing from the estimated cell. The number of pulses present in the real situation is given by

$$N_{Real} = \left[\sum_{i=1}^{N} hist(d_i) \right] + 1 \tag{36}$$

and consequently the number of missing pulses is given by

$$N_{Missing} = N_{Ideal} - N_{Real} \tag{37}$$

The cell quality, Q_c of a deinterleaved cell is defined as

$$Q_C = \frac{N_{Ideal} - N_{Missing}}{N_{Ideal}} = \frac{N_{Real}}{N_{Ideal}} \tag{38}$$

Radar cells with stable, jittered and staggered *PRI* have been generated in a simulation program. Some of the pulses in the cell were purposely dropped and both the cell quality Q_c for the deinterleaved cell as well as the number of missing pulses from that cell are estimated using (37) and (38) respectively. Tables 3-5 show some of the simulation results with the threshold of **hist'** set to 0.8.

Table 3. Stable *PRI* radar, *PRI* =952 μ sec., Observation time = 0.25 sec., $N_{Ideal} \approx N_1 \times \left[\frac{\theta}{PRI_{Frame}} + 1\right]$=263.

Actual number of dropped pulses	$N_{Real} = \left[\sum_{i=1}^{N} hist(d_i)\right] + 1$	Estimated number of missing pulses	Cell Quality Q_C [%]
0	263	0	100.00
5	258	5	98.10
10	253	10	96.20
15	248	15	94.30
20	243	20	92.40
25	238	25	90.49
30	233	30	88.59

Table 4. Jittered *PRI* radar, $\overline{PRI}$ =1111.11 μ sec., Observation time = 0.25 sec., $N_{Ideal} \approx N_1 \times \left[\frac{\theta}{PRI_{Frame}} + 1\right]$=225.

Actual number of dropped pulses	$N_{Real} = \left[\sum_{i=1}^{N} hist(d_i)\right] + 1$	Jitter Fraction (JF %)	Estimated number of missing pulses	Cell Quality Q_C [%]
0	225	4.85	0	100.00
5	220	4.95	5	97.78
10	215	4.90	10	95.56
15	211	4.80	14	93.78
20	205	4.98	20	91.11
25	199	4.89	26	88.44
30	196	4.79	29	87.11

Table 5. Staggered *PRI* radar, *PRI* = 1000, 714.28, 588.25 μ sec., Observation time = 0.25 sec., $N_{Ideal} \approx N_1 \times \left[\frac{\theta}{PRI_{Frame}} + 1\right]$=327.

Actual number of dropped pulses	$N_{Real} = \left[\sum_{i=1}^{N} hist(d_i)\right] + 1$	Estimated number of missing pulses	Cell Quality Q_C [%]
0	326	1	99.69
5	321	6	98.17
10	316	11	96.64
15	311	16	95.11
20	306	21	93.28
25	301	26	92.05
30	296	31	90.52

The number of peaks N_1 in the histogram represents the number of *PRI* values the radar uses during the observation time. Hence, we can determine whether the estimated radar uses a stable, or staggered *PRI*. A jittered *PRI* has $N_1 = 1$ like a stable *PRI* radar but we can estimate the jitter fraction for that radar. It can be seen from Tables 3-5 that the value of Q_c decreases with the actual number of missing pulses. Furthermore, the tables show that there is a good agreement between the estimated number of missing pulses computed using (37) and the actual number of missing pulses. The Q_c calculated from (38) gives a good indication of the quality of the deinterleaved cell. Therefore, the performance of the deinterleaving process can be evaluated and hence actions against radars, with low Q_c could be avoided.

Finally, it is concluded that by applying the proposed method to all the deinterleaved cells, the reliability of the deinterleaver can be evaluated. From the analysis presented previously, the factor of successful processing can thus, be determined as

$$F_s = 1 - \frac{\sum_{i=1}^{N_{Radar\ Cells}} N_{Mis\,sing}(i)}{\sum_{j=1}^{N_{Radar\ Cells}} N_{Ideal}(j)} \qquad (39)$$

where $N_{Radar\ Cells}$ is the number of deinterleaved cells generated at the output of the deinterleaver after a given observation time.

6. SIMULATION STUDIES

This Section describes simulation experiments to verify the accuracy of the on-line measurement of F_s. F_s has been evaluated theoretically using (12) and is plotted in Figure 9. The product of $\hat{F}_P$ and $\hat{F}_E$ which have been obtained using simulations is also shown in Figure 9. There is an excellent agreement between the two values. These values are also very close to the one evaluated using (39).

In Section 2, we have seen that the value of F_P is a function of λ and Ts. Also, as discussed in Section 3, F_E is a function of λ, T_s and T_a. Thus, the factor of successful processing of the *ESM* system is a function of λ, T_s and T_a. Consequently, at constant T_s and T_a, F_s will be a function of λ. The importance of this relation is that, given a minimum acceptable F_s, we can compare this minimum to that computed on-line from (39), to determine whether the arrival rate exceeds the capability of the *ESM* system. If (39) gives value smaller than the acceptable F_s, this is an indication that the *ESM* system is overloaded. This means that the pulse arrival rate is higher than the *ESM* capability, and we should increases the processing capability of the *ESM* system. Moreover, the

minimum acceptable F_s is the threshold used for the figure of merit defined by (40). The relationship $F_s = F_P \times F_E$ can also be applied to determine the highest rate of pulses that the *ESM* system can accept. As seen in Sections II and III, there is an excellent agreement between the theoretical and the simulated results of F_P and F_E. Therefore we can use the product of F_P and F_E, which are functions of λ, T_s and T_a , to plot F_s as a function of λ for different T_s and T_a. This plot is in Figure 10.

In Figure 10, F_s is calculated as a function of λ for two *ESM* systems. These systems have different parameters (T_s and T_a) and we use this plot to determine their capabilities. If the threshold of F_s is, say 85 %, then the capability of the *ESM* system is the value of λ corresponding to that threshold. As an example, the maximum value of λ to achieve F_s greater than or equal to 85 % when the *ESM* parameters are T_s = 4 μ sec and T_a = 60 μ sec is smaller than the same value when the *ESM* parameters are T_s = 3 μ sec and T_a = 50 μ sec. Thus based on the *ESM* parameters and the arrival rate of pulses, It will be easy to determine whether the *ESM* system is functioning within its capability.

7. CONCLUSIONS

A method for evaluating the reliability of a deinterleaver has been proposed and analyzed. The proposed method is based on the *TOA* information of the pulses inside each deinterleaved radar cell. From this analysis we can estimate the number of missing pulses from the deinterleaved cells and consequently evaluate a figure of merit for each cell. The number of missing pulses from the deinterleaved cells is then used to evaluate the factor of successful processing of the *ESM* system. The same factor is derived as a function of the parameters of the *ESM* system and the arrival rate of pulses at the input of the *ESM* system. The simulation results show a good agreement between F_s measured and F_s evaluated from the analytic expression as a function of the parameters of the *ESM* system and the arrival rate of pulses. Thus from F_s, we can estimate the arrival rate of pulses for the given parameters of the *ESM* system. It is of practical use to know the arrival rate. Generally, the capability of the *ESM* system is known and if the arrival rate exceeds this capability, it should signal the *ESM* operator to bring in additional resources.

8. REFERENCES

[1] Schleher, D., Introduction to Electronic Warfare, Artech House, Inc., 1982.
[2] David, C. L., and Holland, P., "Automatic Processing for ESM," IEE Proc. F, Comm., Radar & Signal Processing, 129, (3), pp. 146-151, 1982.
[3] Wiley, R. G., The Interception of Radar Signals, Artech House, Inc., 1982.
[4] Wiley, R. G., The Analysis of Radar Signals, Artech House, 1993.

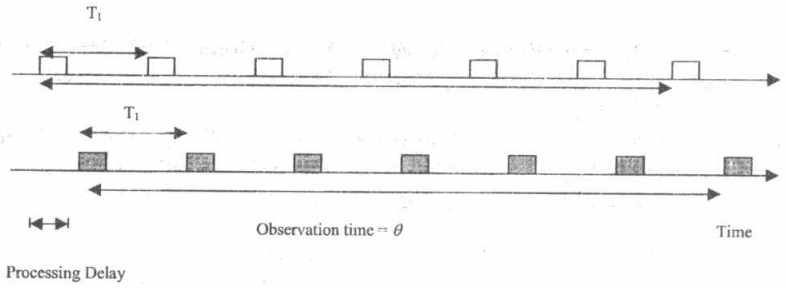

Figure 3. Pulses emitted from one radar in θ , Pulses inside the estimated radar cell in

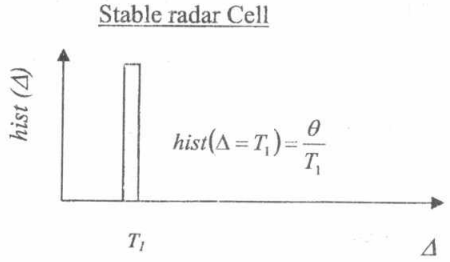

Figure 4. Δ_i -histogram of stable radar

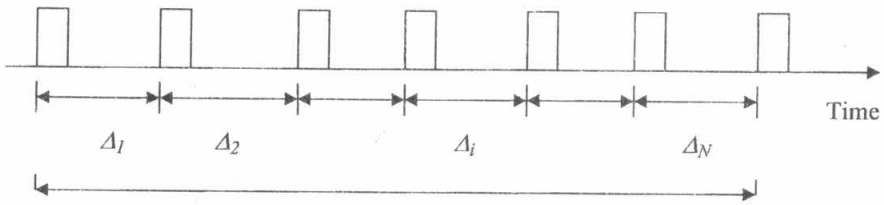

Observation time = θ

Figure 5. Pulses of jittered radar cell

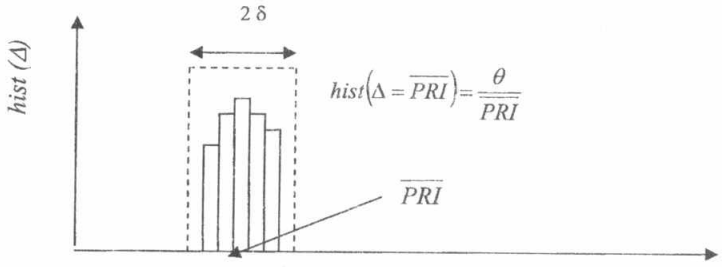

Figure 6. Δ_i - histogram of jittered radar

[5] Wilkinson, D. R., and Watson, A. W., " Use of Metric Techniques in *ESM* Data Processing," IEE Proc. F, Comm., Radar & Signal Processing, 132, (7), pp. 621-625, 1985.

[6] Brolly, C., Alengrin, G., Lopez, J. and Perez, P., "Multi-Hypothesis Method in Pulse Deinterleaving," Proceedings of the SPIE Conference on Radar Processing Technology and Applications III, vol. 3462, pp. 273-282, July 1998.

[7] Chan, Y. T., Chan, F., and Hassan, H. E., "Performance Evaluation of ESM Deinterleaving Using TOA Analysis," The 14th International Conference on Microwave, Radar and Wireless Communications, Vol. 2, pp. 341-350, Poland, May 2002.

[8] Gross, D. and Harris, C., Fundamentals of Queueing Theory, John Willey & Sons, 1974.

[9] Gelenbe, E. and Pujolle, G., Introduction to Queueing Network, John Willey & Sons, 1987.

[10] Kashyap, B. R. And Chaudhry, M. L., An Introduction to Queueing Theory, A & A Publications, 1988.

[11] Gelenbe, E. and Pujolle, G., Signal Theory and Processing, John Willey & Sons, 1986.

[12] El-Ayadi, M. H., El-Barbary, K. and Hassan, H. E. A., "Analysis of the Queueing Behavior of Automatic ESM System," IEEE Transactions on Aerospace and Electronic Systems Vol. 37, No. 3, July 2001.

Figures

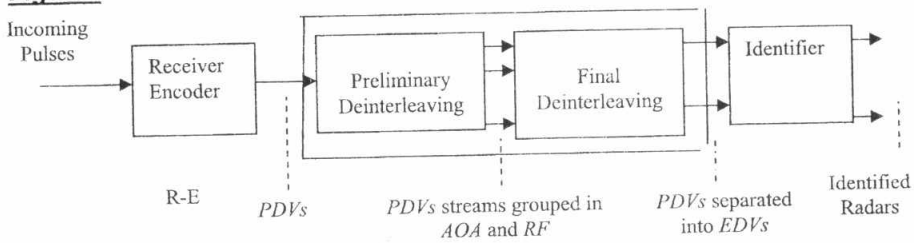

Figure 1. An *ESM* System

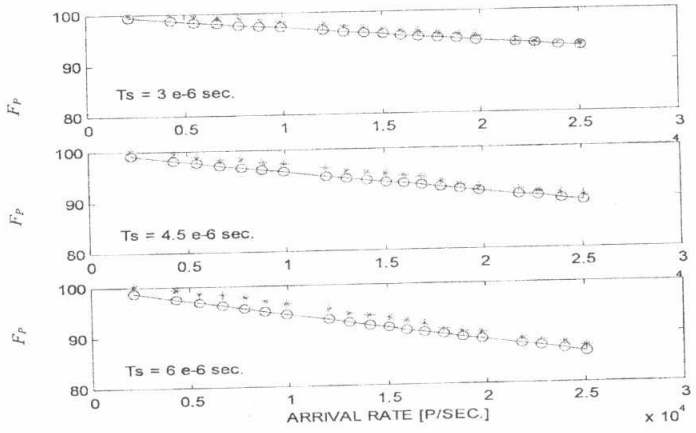

Figure 2. F_P versus the arrival rate, * represent $\hat{F}_P$, ○ represent F_P.

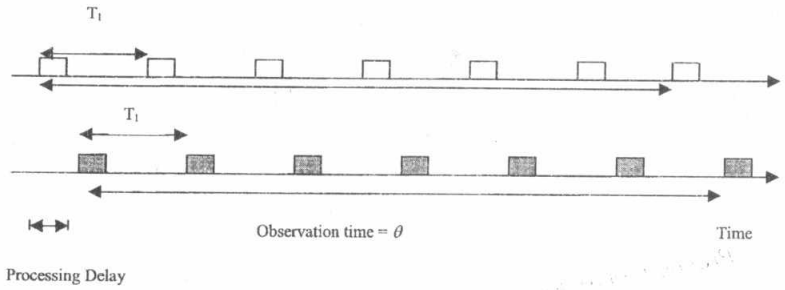

Figure 3. Pulses emitted from one radar in θ , Pulses inside the estimated radar cell in

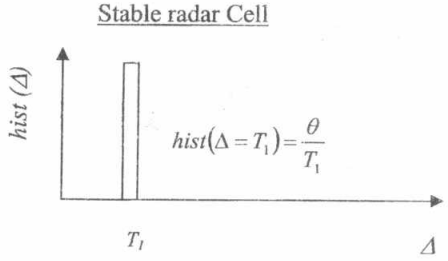

Figure 4. Δ_i -histogram of stable radar

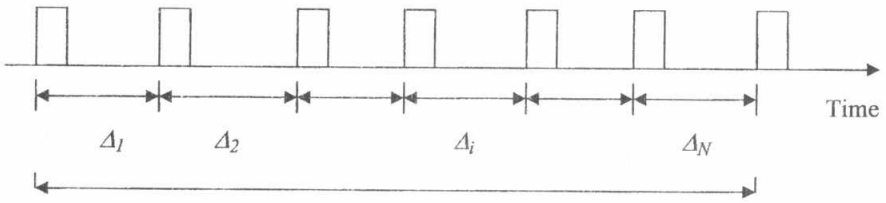

Observation time = θ

Figure 5. Pulses of jittered radar cell

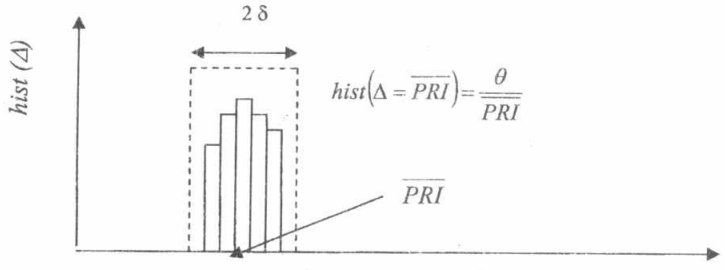

Figure 6. Δ_i - histogram of jittered radar

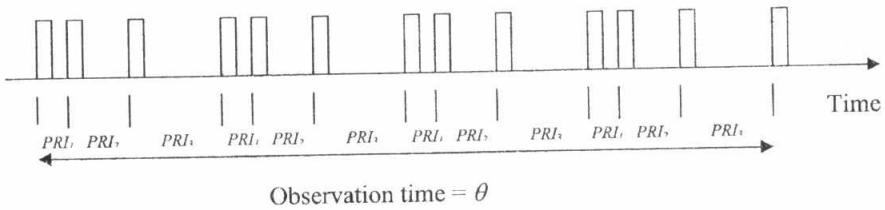

Figure 7. Pulses of stagger radar cell. PRI_1: PRI_2: PRI_3 = 1:2:3

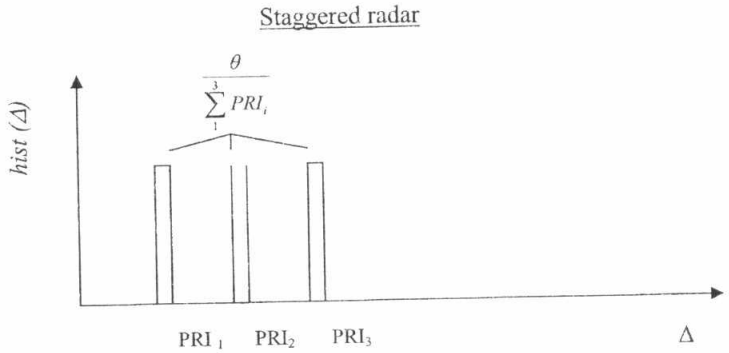

Figure 8. Δ_i histogram of staggered PRI radar

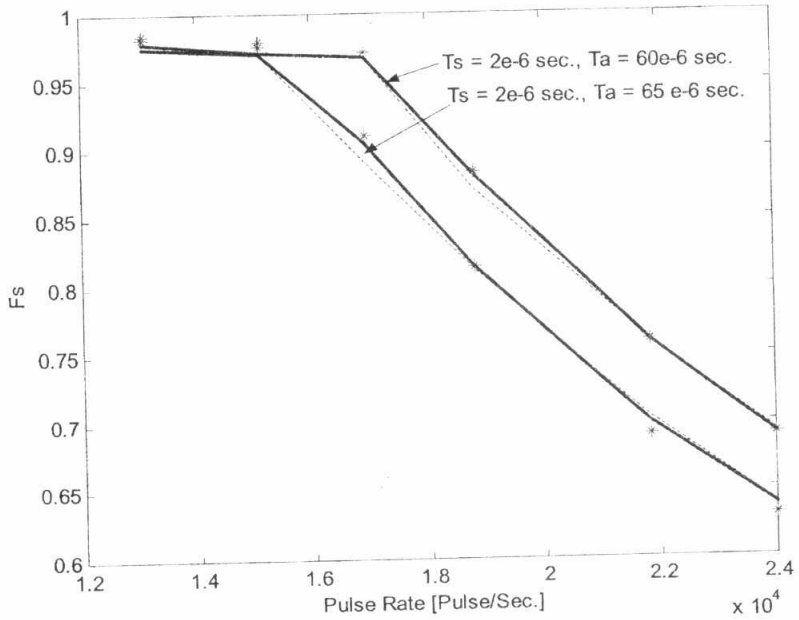

Figure 9. The factor of successful processing Vs the pulse rate,
___ $F_P \times E_E$, ----- $\hat{F}_P \times \hat{F}_E$, *$F_s$ from equation (41)

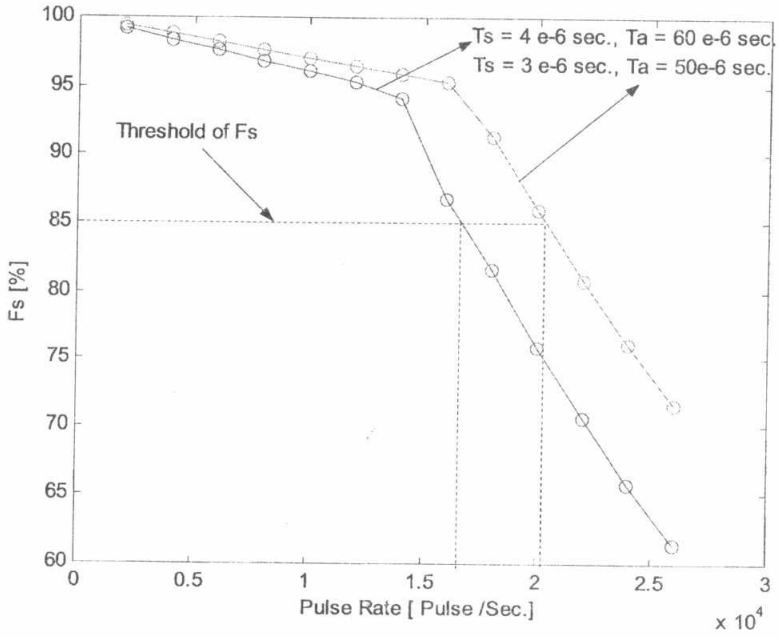

Figure 10. The factor of successful processing as a function of λ.